Journal of Applied Sciences

ISSN 1812-5654

science alert

ANSInet
an open access publisher
http://ansinet.com

Journal of Applied Sciences 7 (22): 3499-3505, 2007
ISSN 1812-5654

Defect and Band Gap Analysis of Real One-Dimensional Layers of Right and Left Handed Photonic Crystals

A.R. Maleki Javan and N. Granpayeh
Faculty of Electrical Engineering, K.N. Toosi University of Technology, Tehran, Iran

Abstract: Recently Left Handed Photonic Band Gap (LHPBG) structures have become the object of intense experimental and theoretical researches due to their novel properties. Most of the early research efforts were concentrated on the analysis of the LHPBG structures consisting of materials with special frequency dependent parameters, such as Drude model for ε and μ of the structure. In this study, first the complete Drude-Lorentz model is introduced for the constitutive parameters of materials and a real one-dimensional structure is analyzed. Then a complete one dimensional left handed photonic band gap with multiple defect states is investigated. For computation of the band structure and transmission spectra of real frequency dependent structures with and without defects, the dispersive finite-difference time-domain method has been used. The effects of number of layers, defects and variation of parameters of spatial dispersion of layers to the band gap of the structure are studied. A multiple channel filtering by variation of the band gap structure is proposed.

Key words: Photonic crystals, left handed materials, band gap structures, negative refractive index materials

INTRODUCTION

Photonic Band Gap (PBG) materials have been intensively investigated experimentally and theoretically during the past two decades (Bowden *et al*., 1993). Conventional dielectric structures with a periodically modulated refractive index exhibit forbidden frequency band gaps. Photons or electromagnetic waves with energy or frequencies within this band gap cannot propagate through these media (Knight *et al*., 1998). PBG structures can be used as a reflector for photon or electromagnetic waves and hence is employed for devices, such as lasers, waveguides, stop band filters and switches (Rhodes, 2003). The band gaps occur due to the Bragg scattering in a periodical dielectric structure with period comparable to the incident photon wavelength (Li and Zhang, 2000). Such Bragg band gaps strongly depend on the incident angle and the polarization of the light (Nusinsky and Hardy, 2006).

Recently left handed materials have been fabricated and the results are in good agreement with the theoretical predictions (Jakšiæ *et al*., 2006; Shelby *et al*., 2001). Left handed (LH) or Negative Refraction Index (NRI) materials must have both negative electric permittivity and magnetic permeability in the same range of wavelengths (Smith *et al*., 2000).

A stake of layers with alternating conventional dielectric and negative refraction materials leads to a new type of PBG corresponding to a zero average refractive index (<n> = 0) gap (Li *et al*., 2003; Yuan *et al*., 2006). A number of unique properties of the zero average refractive index gap on the beam shaping effect has been studied (Shadrivov *et al*., 2003). Such a novel gap is quite different from the conventional Bragg reflection gap and it appears due to a different physics of wave reflection. This gap is independent of scaling and insensitive to the disorder (Wu *et al*., 2003). It has been demonstrated that the edges of the zero averaged refractive index gap in a special structure is insensitive to the incident angle for different wave polarizations, leading to an omni-directional gap (Jiang *et al*., 2003). When the periodicity is broken by introducing a defect into the left handed material, a localized defect mode will appear inside the Bragg gap or zero averaged refractive index gap, which depends on the defect parameters. Defect modes in zero averaged refractive index band gap, contrary to the Bragg ones are weakly dependent on the angle and polarization of the incident wave (Jiang *et al*., 2003; Shadrivov *et al*., 2004).

In previous investigations the models for the simulation of constitutive parameters of the materials were simply the same. But since the origins of phenomena to create these negative parameters are different, therefore their model must be different. The Drude-Lorentz model describes very well the behavior of these parameters.

Corresponding Author: A.R. Maleki Javan, Faculty of Electrical Engineering, K.N. Toosi University of Technology, Tehran, Iran

In this study, variations of the transmission characteristics of the real dispersive one dimensional left handed photonic band gap structure with defects are studied by Finite Difference Time Domain (FDTD) method. The effects of variations of the parameters of the layers and defects of these materials, by assuming the Drude-Lorentz model for the frequency dependent permittivity and permeability are analyzed. A one-dimensional band gap structure that has the same response to both TE and TM polarizations is proposed. The properties of the defect modes inside the zero averaged index band gap structure are investigated. Based on these theoretical results, a multi channel filter is introduced.

Analysis of photonic crystals with constant permittivity and permeability: Some periodic structures have band gaps for certain ranges of propagation directions and/or TE or TM modes. If a structure has band gaps for all ranges of propagation directions, it demonstrates a complete band gap or omni-directional gap.

In this study, the propagation of the electromagnetic waves in the structure of Fig. 1, an infinite one-dimensional periodic structure consisting of two different layers of materials with periodicity in the z direction, is studied. For TE polarized electromagnetic waves, which the electric field component is parallel to the layers, the wave equation is given by:

$$\frac{\partial^2 E(x,z,t)}{\partial x^2}+\frac{\partial^2 E(x,z,t)}{\partial z^2}= \frac{n^2(z)}{c^2}\frac{\partial^2 E(x,z,t)}{\partial t^2}+\frac{1}{\mu(z)}\frac{\partial \mu}{\partial z}\frac{\partial E(x,z,t)}{\partial z} \quad (1)$$

where:

$$n(z)=\sqrt{\varepsilon(z)\mu(z)}$$

is the periodic refractive index with period of unit cell width, a.

Propagation of electromagnetic waves in photonic crystals obey the Bloch's conditions and are characterized by the Bloch wave number, k_b, expressed as (Li *et al*., 2003):

$$E(x,z+a)=E(0,z)\exp(ik_x x+ik_b a) \quad (2)$$

where:

k_b = The Bloch wave number.
k_x = The x-component of wave number.
$k_{x=0}$ = The normal incident.

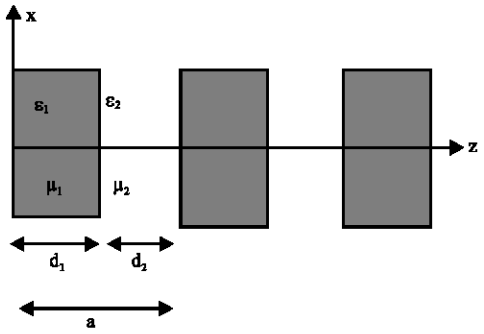

Fig. 1: Structure of a one-dimensional photonic crystal consisting of two different alternative layers

Now, the oblique monochromatic electromagnetic fields, as the solutions of Eq. 1 in different layers of the structure of Fig. 1 are derived. By satisfying the boundary conditions, at the interface of media 1 and 2 and considering the Bloch's condition, the relation for the TE polarization case is given by Li *et al*. (2003):

$$2\cos(k_b a)=2\cos(k_{1z}d_1)\cos(k_{2z}d_2) -\left(\frac{k_{2z}\mu_1}{k_{1z}\mu_2}+\frac{k_{1z}\mu_2}{k_{2z}\mu_1}\right)\sin(k_{1z}d_1)\sin(k_{2z}d_2) \quad (3)$$

where, a is the width of the unit cell $(a=d_1+d_2)$, $k_{jz}=\sqrt{k_j^2-k_x^2}$ are the z component of the wave vector in the first (j = 1) and the second (j = 2) medium and

$$k_j=\frac{\omega n_j}{c}$$

is the wave number in each media with refractive index of n_j, ω is the wave angular frequency and c is the speed of light in free space.

Similarly, the dispersion relation of the TM polarized wave is derived by replacing μ by ε in Eq. 3. Solutions of this dispersion relation demonstrate the behavior of the structure. If k_x and k_b are real, the Bloch wave propagates through the periodic structure, whereas if k_x or k_b are imaginary, the wave propagation is not possible and there will be a band gap in the transmission spectrum of the structure. It has been shown that the gap width of a one dimensional photonic crystal strongly depends on the angle of incident light. Moreover, the band gap is sensitive to polarization. A complete band gap occurs if for all real k_x, k_b remains complex, which the wave propagation in this structure is inhibited (Li and Zhang, 2000).

Now, if media 2 is considered as a LHM, the only difference in the derivation of Eq. 3 is that the sign of the wave vector in this medium must be reversed. This structure may have particular property with new band gap when the condition of zero average refraction indices of Eq. 4 is satisfied:

$$< n >= \frac{1}{a}\int_0^a n(z)dz = 0 \quad (4)$$

In particular, the frequency corresponding to the zero average refraction index gap is independent of the width of the unit cell, while all Bragg gaps are scaled with the width of unit cell. Based on the results derived in (Shadrivov *et al*., 2005), a one dimensional periodic structure composed of unit cells with two layers of conventional and LH material with particular parameters will possesses a complete band gap for one polarization. However, there is no complete band gap for the other polarization.

Shadrivov *et al*. (2005) have shown that in a three layer periodic structure with cell property of two LHM layers with the same thickness and dual constitutive parameter ($\varepsilon_{1,2} \Leftrightarrow \mu_{2,1}$) surrounding a conventional dielectric, a complete band gap for both polarizations exits.

Analysis of dispersive left handed photonic crystals: Most of the early researches were concentrated on the LHPBG structures consisting of materials with special frequency dependent parameters. In this study, real dispersive materials with frequency dependent parameters are considered.

The left handed materials have structures, which are usually printed or drilled onto appropriate substrates (for example split ring resonators and fine wires). Their characteristic size is small compared to the wavelength. The material behaves with averaged effective properties describable by ε and μ. It is evident that these parameters directly depend on the shape, kind and type of the materials of the structure (Jakšiae *et al*., 2006). The inherent feature of these materials is their frequency dependent dispersion and losses. Materials with negative refractive index, i.e., simultaneously negative ε and μ are dispersive. The Drude-Lorentz model describes very well the constitutive parameters of these materials. In frequency domain, the effective permittivity $\varepsilon(\omega)$ and permeability $\mu(\omega)$ can be expressed as (Ramakrishna, 2005; Smith *et al*., 2000):

$$\varepsilon(\omega) = \varepsilon_0\left[1 - \frac{\omega_{pe}^2}{\omega^2 + i\Gamma_e\omega}\right]$$
$$\mu(\omega) = \mu_0\left[1 - \frac{\omega_{pm}^2 - \omega_{mo}^2}{\omega^2 - \omega_{mo}^2 + i\Gamma_m\omega}\right] \quad (5)$$

where:

ω_{pe} and ω_{pm} = The effective electric and magnetic plasma frequencies, respectively.

ω_{mo} = Magnetic resonance frequency.

ω = The angular frequency of the wave.

These models include losses represented by the parameters Γ_e and Γ_m and can also be modified for implementation of the nonlinear effects (Zharov *et al*., 2003). From Eq. 5, it is clear that these materials have a limited frequency bands in which their constitutive parameters are negative, therefore, some new methods are required for analysis of these structures. An analytical computation of the band structure and transmission spectra of LHPBG with dispersive parameters and defect is difficult. The FDTD method is a powerful method that can simulate the complex structures.

First, the PBG structure of Fig. 1 consisting of two cascaded negative and positive refractive index slabs is considered. The one dimensional FDTD method is used to simulate the behavior of the structure. At the beginning we have selected the same Drude model for constitutive parameters which means $\omega_{mo} = 0$ (Ziolkowski, 2003; Young and Nelson, 2001). At both ends of simulation windows, absorbing boundary conditions are used. The spatial steps is set at $\Delta z = \lambda/100$, where λ is the free space wavelength. The time step Δt is set at $\Delta t = 0.95\Delta z/c$, where c is the speed of light. The input wave is a narrow Gaussian pulse with duration of $\lambda/10$ in order to obtain the impulse response of the structure, while 1000 spatial steps and 30000 time steps are considered.

The transmittance of the structure is shown in Fig. 2. The dashed line gives the transmittance of a stack of eleven unit cells with $\Gamma_e = \Gamma_m = 3.75\times10^{-4}\ \omega_{pe,\,pm}$ and solid line gives it for $\Gamma_e = \Gamma_m = 0$.

The $<n> = 0$ condition occurs at about 2.72 GHz and the band gap width for both cases is 1.25GHz. For the low loss structures, as are fabricated recently, the loss has a very weak effect on the band gaps. Therefore, in the next simulations, the values of Γ_e and Γ_m are assumed to be zero.

Deeper band gaps are induced for higher number of unit cells. The number of ripples in the pass band is equal to the number of unit cells. These ripples are the frequencies in which the complete transmissions occur. Therefore, to obtain a flat pass band and deeper band gap, the number of unit cells must be increased. The effects of different parameters of effective permittivity and permeability on the band gap of the structure under study are shown in Fig. 3.

It is clearly shown that the edges of zero average refractive index band gap is a function of magnetic resonance, electric and magnetic-plasma frequencies. The width of bandgap depends on the difference of electric and magnetic plasma frequencies. Variations of magnetic resonance frequency, ω_{mo}, shift the upper edge of the band gap. Since ω_{mo} is much lower than ω_{mp}, we have used the same Drude model for the constitutive parameters ε

and μ (Ramakrishna, 2005). When effective electric and magnetic plasma frequencies are equal, all the band gaps are disappeared due to the matching of two layers.

Now, a band gap structure constituting of M-unit cells, (Fig. 4) is selected to be analyzed. Each cell is composed of three layers. One of these layers is a conventional dielectric (air) which is sandwiched by other two layers. These two layers have a left handed nature with dual constitutive parameters. All the layers have the same thickness d_1 except the conventional dielectric in the middle which is d_2. The defect at the center of the structure is a dielectric layer, as d epicted in Fig. 4. The width of this defect layer is $d_3 = d_2 (1-\Delta)$, where Δ is the normalized defect size. Due to the symmetric parameters, this structure has the same response to both polarizations.

A normal incident Gaussian beam is launched to the structure for both polarizations. The structure parameters are $\varepsilon_d = \mu_d = 1$, $\varepsilon_1(\omega) = 1-5^2/\omega^2$, $\mu_1(\omega) = 1-3^2/\omega^2$, $\varepsilon_2 = \mu_1$ $\mu_2 = \varepsilon_1$, $d_1 = \lambda/20$ and $d_2 = \lambda/10$, with $\lambda = 10$ cm.

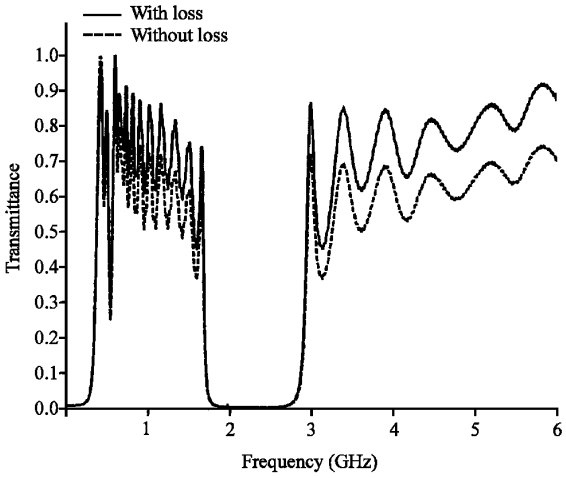

Fig. 2: Transmittance of eleven unit cells with alternate layers of air (12 mm thick) and LHM material (6 mm thick) with effective ε(ω) and μ(ω) given by Eq. 5 ($f_{pe} = \omega_{pe}/2\pi = 3$GHz, $f_{pm} = \omega_{pm}/2\pi = 5$GHz)

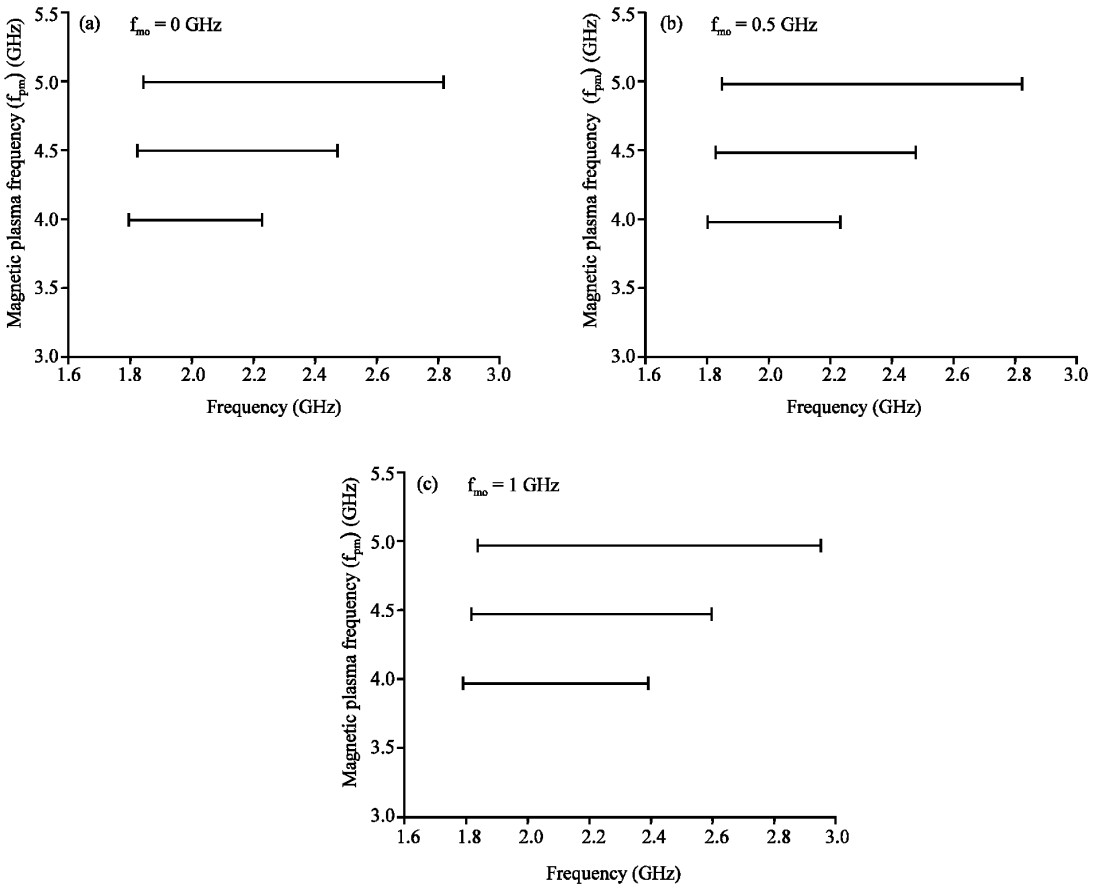

Fig. 3: Variation of zero averaged refractive index band gap of seventeen unit cells with alternate layers of air (12 mm thick) and LHM (6 mm thick) with effective ε(ω) and μ(ω) given by Eq. 5 for different values of magnetic plasma and magnetic resonance frequencies. (a) f_{mo} = 0GHz, (b)f_{mo} = 0.5 Ghz and (c) f_{mo} = 1GHz, with f_{pe} = 3GHz

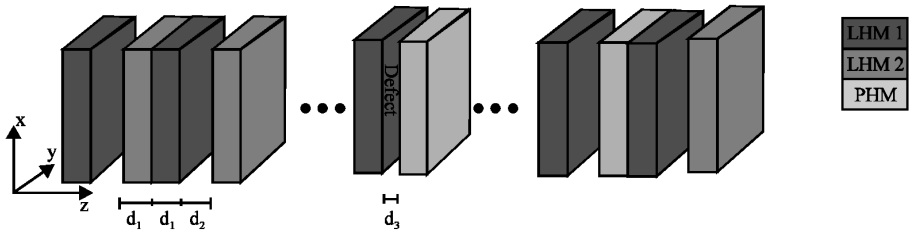

Fig. 4: A 1D complete band gap left handed structure consisting of layers of LHM, conventional dielectric or positive handed material (PHM) and one defect layer in the middle

RESULTS AND DISCUSSION

The FDTD method predicts the electric field intensities at all points of the simulation window. The transmittance spectra of the structure of Fig. 4 with seven unit cells, with and without defect are demonstrated in Fig. 5. Three possible kinds of band gap are shown in Fig. 5. One is a Bragg band gap that generally appear in photonic crystals. The other is zero averaged (<n> = 0) band gap, which is particularly created due to layers of alternating conventional dielectric and left-handed materials.

Another band gap exists in the spectrum, which is called 'zero-order stop band' and appeared just above zero frequency (Fig. 5). Existence of this band gap is determined by appropriate selection of the parameters of the structure (Ye *et al*., 2005). Also defect mode has been created inside the zero averaged and Bragg band gaps. Comparison of Fig. 5 and 6 approves that the defect mode inside the zero averaged band and the edges of the zero averaged band gap is independent of the scaling. Also, it is shown that it has a weak dependence on the incident angle of the input wave (Jiang *et al*., 2003).

Deeper band gaps are induced for higher number of unit cells, as depicted in Fig. 7. Consequently, induced band gaps over a wide range of frequency can be achieved, which the effect can be applied for the perfect reflectors for both polarizations.

Design of band-reject filters are accessible by these structures, the description of which will be published in a new paper. Variation of the normalized defect size, Δ, shifts the defect mode. With special parameters the defect mode appears in the zero averaged refractive index or Bragg gap, but it does not always appear simultaneously in all gaps. Variations of transmittance spectra and shift of the defect mode with different normalized defect size, Δ are shown in Fig. 8.

The width and peak frequency of the defect mode inside the zero averaged gap vary with number of cells of LHPBG structure (Fig. 9). When the number of unit cells

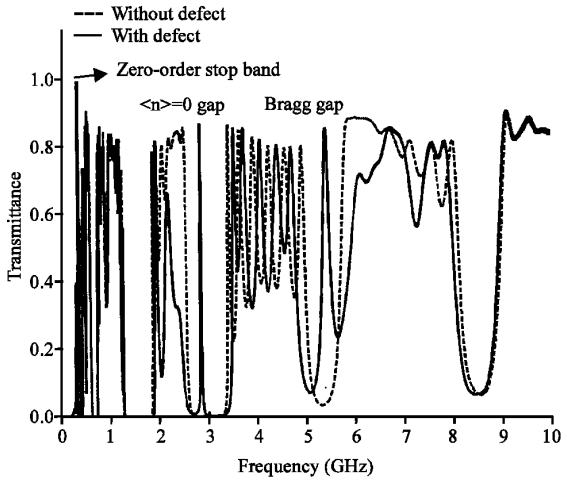

Fig. 5: Transmittance of seven unit cells of Fig. 4, for the structure with normalized defect size of Δ = 0.8 (solid line) and without defect (dashed line)

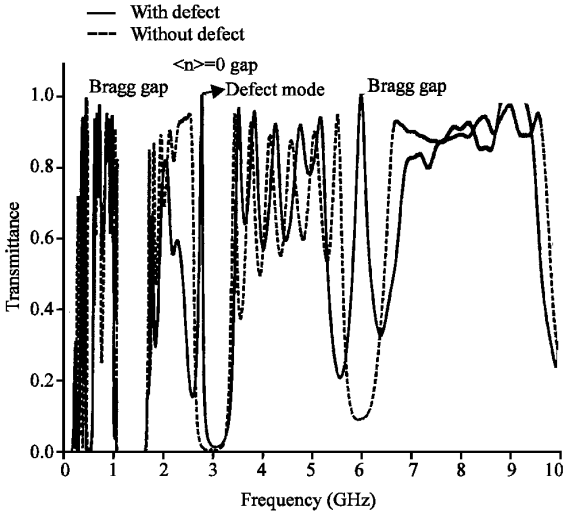

Fig. 6: Transmittance of seven unit cells of Fig. 4, for the structure with normalized defect size of Δ = 0.8 (solid line) and without defect (dashed line) that unit cell is scaled by 3/4

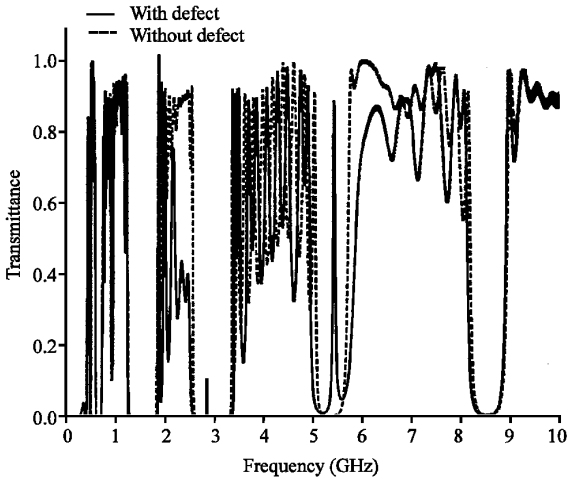

Fig. 7: Transmittance of eleven unit cells of Fig. 4, for structure with normalized defect size of $\Delta = 0.8$ (solid line) and without defect (dashed line)

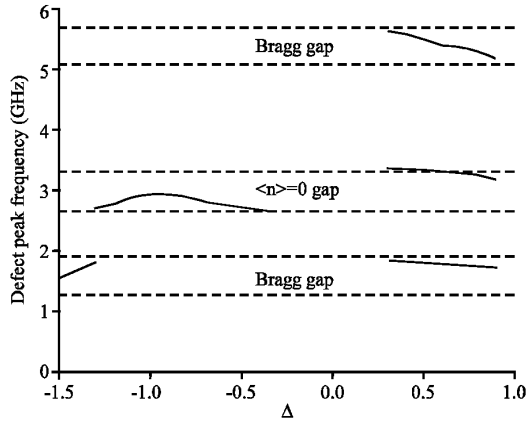

Fig. 8: Frequency spectrum of the defect modes for seven unit cells of Fig. 4 versus the normalized defect size Δ

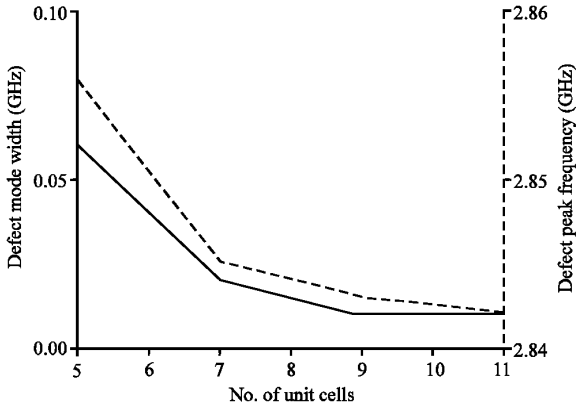

Fig. 9: Half maximum width and peak frequency of the defect mode inside the zero averaged gap versus the number of unit cells of Fig. 4

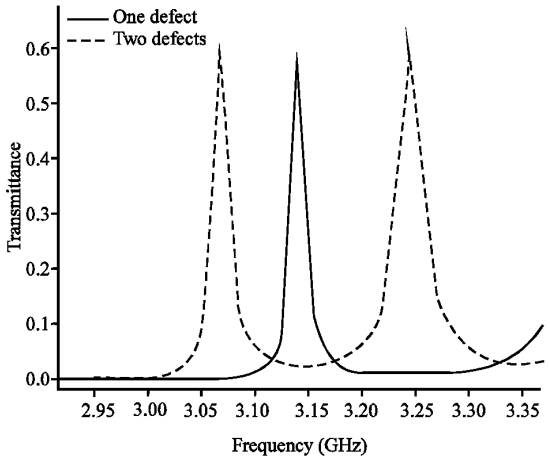

Fig. 10: Defect modes inside <n> = 0 gap for 17 unit cells of Fig. 4, with d_1 = 8 mm, d_2 = 16 mm and d_{defect} = 26 mm. Position of the defect layer for single defect structure is in the 9th and those of double defects are in 9th and 11th cells

increases, the defect mode becomes less visible. The defect mode weakly depends on the scaling and polarization. The defect mode is useful for design of high quality filters.

The simulation can be extended to the study of the properties of multiple defect layers. By increasing number of defect in the structure of Fig. 4, the number of defect modes in the <n>=0 gap increases.

Figure 10 compares the defect modes of structures with one and two defect layers. This phenomenon may be useful in the design of multiple channel filters.

CONCLUSIONS

In this study, the transmittance spectrum of the one dimensional left handed photonic band gap structure with multiple defects has been analyzed by dispersive FDTD. The band gap spectra of the one dimensional multi layer slabs of conventional dielectric and left handed materials, with and without defect were derived. Three different band gaps of zero order, Bragg and zero average refractive index can be displayed in the spectrum of the multi layer slabs with particular parameters. The width of the zero average refractive index band gap depends on the difference between the electric and magnetic plasma frequency, not their direct values. Deeper band gap and flatter pass band are induced for higher number of units. The edges of the zero average refractive index band gap are function of effective permittivity and permeability parameters and less dependent on the scaling of the layer

thicknesses. Increasing the magnetic resonance frequency, ω_{mo} increases the upper edge of the band gap. Since ω_{mo} is much lower than magnetic plasma frequency, ω_{pm} the models without ω_{mo} can also give acceptable results. When effective electric and magnetic plasma frequencies are equal all band gaps are closed due to the matching of layers. Properties of the defect modes are demonstrated. Depending on the defect size, the defect mode may appear in zero average index or Bragg band gap. The edges of the band gaps and the defect modes depend weakly on frequency scaling. A particular structure may have the same response for both polarizations. We have studied properties of single and multiple defects. When the total number of layers of a structure with defect is more than 10, the defect mode width and the defect peak frequency remain constant. Multiple defect modes are produced when multiple defect layers are periodically placed in the structure. As the periods of the defect layers increase, the resonance transmission modes locate symmetrically in the band gap region. The properties of these structures provide possible applications, such as multiple channel omni-directional filtering.

ACKNOWLEDGMENT

The authors would like to thank Iran Telecommunication Research Center (ITRC) for the financial support of this project.

REFERENCES

Bowden, C.M., J.P. Dowling and H.O. Everitt, 1993. Development and applications of materials exhibiting photonic band gaps. J. Opt. Soc. Am., 10: 280-413.

Jakšiæ, Z., N. Dalarsson and M. Maksimovic, 2006. Negative refractive index metamaterials principles and applications. Microwave Rev., 12: 36-49.

Jiang, H.T., H. Chen, H.Q. Li and Y.W. Zhang, 2003. Omnidirectional gap and defect mode of one-dimensional photonic crystals containing negative-index materials. Applied Phys. Lett., 83: 5386-5388.

Knight, J.C., J. Broeng, T.A. Birks and P.St.J. Russell, 1998. Photonic band gap guidance in optical fibers. Science, 282: 1476-1478.

Li, Z.Y. and Z.Q. Zhang, 2000. Fragility of photonic band gaps in inverse-opal photonic crystals. Phys. Rev. B, 62: 1516-1519.

Li, J., L. Zhou, C.T. Chan and P. Sheng, 2003. Photonic band gap from a stack of positive and negative index materials. Phys. Rev. Lett., 90. 083901, 1-4.

Nusinsky, I. and A. Hardy, 2006. Band gap analysis of one dimensional photonic crystal and conditions for gap closing. Phys. Rev. B, 73: 104-125.

Ramakrishna, S.A., 2005. Physics of negative refractive index materials. Rep. Prog. Phys., 68: 449-521.

Rhodes, W.T., 2003. Photonic Crystals Physics, Fabrication and Application. Springer, Berlin.

Shadrivov, I.V., A. Sukhorukov and Y. Kivshar, 2003. Beam shaping by a periodic structure with negative refraction. Applied Phys. Lett., 82: 3820-3822.

Shadrivov, I.V., N.A. Zharova, A.A. Zharov and Y.S. Kivshar, 2004. Defect modes and transmission properties of left-handed bandgap structures. Phys. Rev. E, 70: 046615, 1-6.

Shadrivov, I.V., A. Sukhorukov and Y. Kivshar, 2005. Complet band gap in one-dimensional left-handed periodic structures. Phys. Rev. Lett., 95: 193903.

Shelby, R., D.R. Smith and S. Schultz, 2001. Experimental verification of a negative index of refraction. Science, 292: 77-79.

Smith, D.R., W.J. Padilla, D.C. Vier, S.C. Nemat-Nasser and S. Schultz, 2000. Composite medium with simultaneously negative permeability and permittivity. Phys. Rev. Lett., 84: 4184-4187.

Wu, L., S. He and L. Shen, 2003. Band structure for a one-dimensional photonic crystal containing left-handed material. Phys. Rev. B, 67: 103-235.

Ye, Z., J. Zheng, Z. Wang and D. Liu, 2005. Characteristics of band structures in 1D photonic crystals containing alternate left-right handed materials. Solid State Commun., 136: 495-498.

Young, J.L. and R.O. Nelson, 2001. A summary and analysis of fdtd algorithms for linearly dispersive media. IEEE Antennas Propagat. Mag., 43: 61-77.

Yuan, Y., L. Ran, J. Huangfu, H. Chen, L. Shen and J. Kong, 2006. Experimental verification of zero order bandgap in a layered stack of left-handed and right-handed materials. Opt. Exp., 14: 2220-2227.

Zharov, A., I. Shadrivov and Y. Kivshar, 2003. Nonlinear properties of left-handed metamaterials. Phys. Rev. Lett., 91: 037401, 1-4.

Ziolkowski, R.W., 2003. Pulsed and CW Gaussian beam interactions with double negative metamaterial slabs. Opt. Exp., pp: 662-681.